





Article

Parameter Uncertainty Analysis of the SWAT Model in a Mountain-Loess Transitional Watershed on the Chinese Loess Plateau

Fubo Zhao ¹ , Yiping Wu ^{1,*} , Linjing Qiu ¹, Yuzhu Sun ¹, Liqun Sun ² , Qinglan Li ², Jun Niu ³  and Guoqing Wang ⁴

¹ Department of Earth and Environmental Science, School of Human Settlements and Civil Engineering, Xi'an Jiaotong University, Xi'an 710049, China; zfubo789@163.com (F.Z.); qiulinjing@mail.xjtu.edu.cn (L.Q.); sunyuzhu12@xjtu.edu.cn (Y.S.)

² Shenzhen Institutes of Advanced Technology, Chinese Academy of Sciences, Shenzhen 518055, China; lq.sun@siat.ac.cn (L.S.); ql.li@siat.ac.cn (Q.L.)

³ Center for Agricultural Water Research in China, China Agricultural University, Beijing 100083, China; niuj@cau.edu.cn

⁴ Nanjing Hydraulic Research Institute, Nanjing 210029, China; guoqing_wang@163.com

* Correspondence: rocky.ypwu@gmail.com or yipingwu@xjtu.edu.cn

Received: 12 April 2018; Accepted: 22 May 2018; Published: 25 May 2018



Abstract: Hydrological models play an important role in water resource management, but they always suffer from various sources of uncertainties. Therefore, it is necessary to implement uncertainty analysis to gain more confidence in numerical modeling. The study employed three methods (i.e., Parameter Solution (ParaSol), Sequential Uncertainty Fitting (SUF2), and Generalized Likelihood Uncertainty Estimation (GLUE)) to quantify the parameter sensitivity and uncertainty of the SWAT (Soil and Water Assessment Tool) model in a mountain-loess transitional watershed—Jingchuan River Basin (JCRB) on the Loess Plateau, China. The model was calibrated and validated using monthly observed streamflow at the Jingchuan gaging station and the modeling results showed that SWAT performed well in the study period in the JCRB. The parameter sensitivity results demonstrated that any of the three methods were capable for the parameter sensitivity analysis in this area. Among the parameters, CN2, SOL_K, and ALPHA_BF were more sensitive to the simulation of peak flow, average flow, and low flow, respectively, compared to others (e.g., ESCO, CH_K2, and SOL_AWC) in this basin. Although the ParaSol method was more efficient in capturing the most optimal parameter set, it showed limited ability in uncertainty analysis due to the narrower 95CI and poor P-factor and R-factor in this area. In contrast, the 95CIs in SUF2 and GLUE were wider than ParaSol, indicating that these two methods can be promising in analyzing the model parameter uncertainty. However, for the model prediction uncertainty within the same parameter range, SUF2 was proven to be slightly more superior to GLUE. Overall, through the comparisons of the proposed evaluation criteria for uncertainty analysis (e.g., P-factor, R-factor, NSE, and R²) and the computational efficiencies, SUF2 can be a potentially efficient tool for the parameter optimization and uncertainty analysis. This study provides an insight into selecting uncertainty analysis method in the modeling field, especially for the hydrological modeling community.

Keywords: GLUE; hydrological model; ParaSol; SUF2; uncertainty analysis

1. Introduction

Watershed systems are complex due to multiple influencing factors (e.g., climate, land use, and other anthropogenic disturbances), and an accurate prediction of the hydrological processes

is indispensable to watershed management [1,2]. Hydrological models have been developed and applied to mathematical representation of hydrological processes, because they can improve the understanding of the impact of natural and anthropogenic disturbances on hydrological features and forecast water resource changes, thus supporting decisions in water resource management [3–5]. However, the model simulation can be highly uncertain due to the defects of the model itself and the complexities of the watershed system, which is now a big concern in the hydrological modeling community [6–9]. Without a realistic assessment of model uncertainty, it is hard to gain confidence in modeling tasks, such as evaluating the responses of the water cycle to future shifts of climate and land use [10]. Therefore, the uncertainty analysis is quite necessary to improve the accuracy and credibility of hydrological simulation.

Uncertainties in hydrological modeling are associated with three possible sources: input data, such as the precipitation data, who can alter the hydrological modeling procedure and simulation results directly (e.g., surface runoff); model structure, which is mainly caused by the assumptions and simplification of the model; and model parameters [6,11–13]. Among these three sources, parameter uncertainty is the most common but relatively easy to control through appropriate calibrations [14]. In general, there exist numerous key parameters in a certain watershed, depicting watershed properties and hydrological processes. These parameters are usually difficult to measure directly, and they are generally derived from the empirical estimation and literature reference, which may introduce uncertainties into the modeling system [12,15,16]. In addition, parameters obtained from calibration are also affected by several factors such as correlations among parameters, sensitive or insensitive in parameters, spatial and temporal scales and statistical features of model residuals, and these may lead to so-called equifinality [17,18].

Numerous studies have focused on parameter uncertainty issues in the hydrological modeling [1,10,19–23]. Several techniques for addressing model uncertainty have been proposed over recent decades. Among those, Parameter Solution (ParaSol) [24], sequential uncertainty fitting (SUFI2) [25], and generalized likelihood uncertainty estimation (GLUE) [26] are three robust ones in the parameter sensitivity and uncertainty analysis in the hydrological simulation [12,14,27,28]. In recent years, there have been a number of studies involving uncertainty analysis using these three methods as well as comparisons of the capabilities for the methods in hydrological simulation and uncertainty analysis [12,14,27,29]. However, the key parameters' identification and the magnitude of their uncertainties vary with the study area/location; it is, therefore, necessary to implement the parameter sensitivity and uncertainty analysis before further hydrological analyses, especially in some distinctive watersheds. The present study aimed to apply these three methods to a distributed hydrological model—SWAT (Soil and Water Assessment Tool) [30]—a physically based distributed hydrological model, which has been increasingly applied to simulate most of the key hydrological processes and assess the water resource management at the watershed scale. We took a typical mountain-loess transitional watershed (Jingchuan River Basin, JCRB) on the Loess Plateau as a case study to: (1) examine the performance and feasibility of SWAT in simulating the streamflow in the JCRB; (2) implement the sensitivity and uncertainty of the parameters using ParaSol, SUFI2, and GLUE; (3) compare the capabilities of these three methods in the parameter uncertainty analysis.

2. Materials and Methods

2.1. Study Area

The JCRB (Figure 1), controlled by the Jingchuan gaging station, lies in the western part of the Jinghe River Basin (106°11'~107°21' E, 35°15'~35°45' N). The JCRB is a mountain-loess transitional zone (Figure 1) with a total area of 3164 km². In this basin, 39% is mountainous/rocky terrain, which is mainly located in the high-elevation (>2000 m) area, while 61% is loess area [31]. The region is controlled by the continental climate, which is hot and humid in summer and cold and dry in winter. The mean annual temperature and precipitation is 8.8 °C and 475 mm in the loess area, and 6.5 °C

and 614 mm in the mountainous area, respectively [31]. Topographically, the elevation drops from the mountainous area to the loess area with a range of 2898 to 1022 m. The major land use and land cover (LULC) types of this region are forest, cropland, and grassland. The forests are mainly distributed in the mountainous area, whereas the grasslands and croplands are mainly in the loess area. The dominant soil type of the JCRB is Cambisols (Figure 1), which is mainly distributed in the loess area.

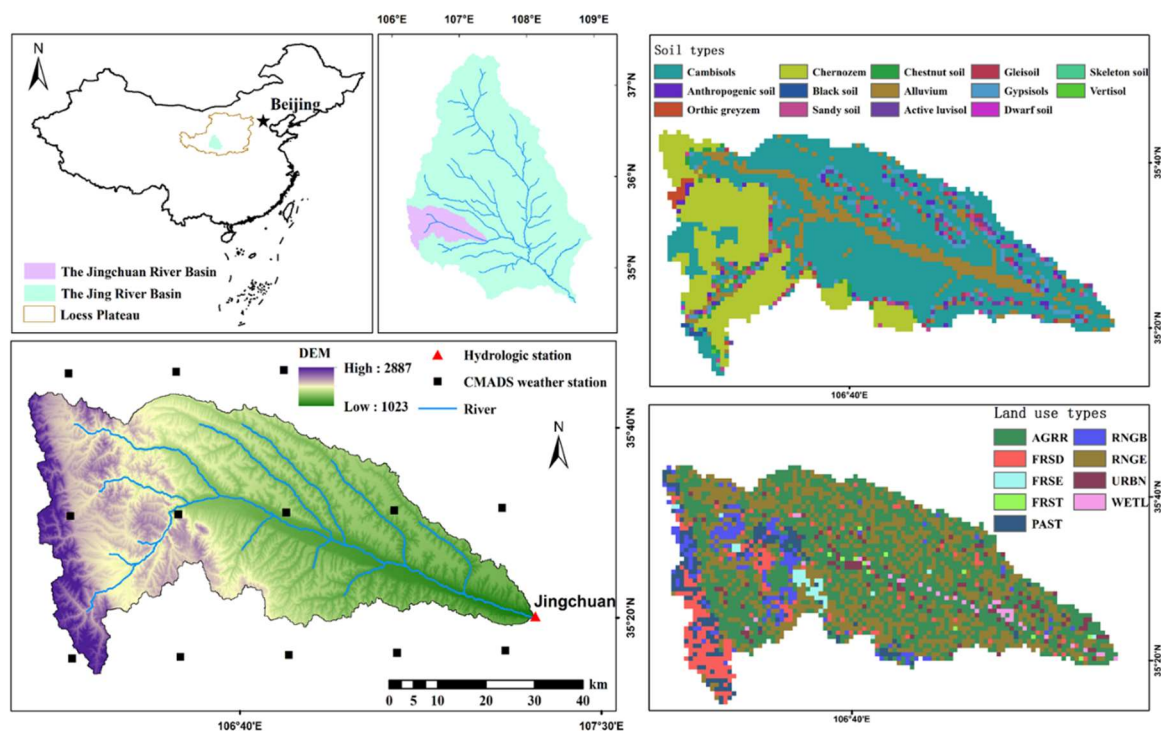


Figure 1. DEM, soil types, and land use types of the Jingchuan River Basin (JCRB).

2.2. Model Description

The SWAT model is a continuous, spatially distributed simulator developed to assist water resource managers in predicting impacts of land management practices on water, sediment, and agricultural chemical yields [30,32]. Fundamentally, the water cycle simulated by SWAT is based on the water balance, whose mathematical equation was reported by Neitsch [32]. The SWAT model is operated at the hydrologic response unit (HRU), which consists of same land use, management, and soil characteristics. The model has been successfully applied around the world for addressing numerous watershed issues under climate shifts and human activities [32,33]. Major outputs of SWAT include surface runoff, baseflow, lateral flow, evapotranspiration (ET), soil water, and water yield.

2.3. Model Input and Setup

The SWAT model requires several specific information such as Digital Elevation Map (DEM), weather, soil properties, and land use and cover types [34]. The DEM with a 90-m resolution was from Shuttle Radar Topography Mission (SRTM). The soil and LULC maps (1 km × 1 km) were from the Ecological and Environmental Science Data Center for West China (<http://westdc.westgis.ac.cn>). The daily meteorological data from 2008 to 2014 were from the China Meteorological Assimilation Driving Datasets for the SWAT model Version 1.1 (CMADS V1.1, <http://www.cmads.org>), which was developed by Dr. Xianyong Meng from the China Institute of Water Resources and Hydropower Research (IWHR) and has received worldwide attention [35]. The CMADS V1.1 provides daily precipitation, maximum/minimum temperature, relative humidity, wind speed, and solar radiation. In this study, to ensure that an equilibrium state is attained before the actual simulation (that is,

the year of 2008), we took both the year 2006 and 2007 as the warm-up period using the actual weather information in this area. The Geographic Information System (GIS) interface was used to delineate the watershed, resulting in 30 sub-basins and 813 HRUs. The average monthly runoff data from 2008 to 2012 were obtained from the Yellow River Hydrology Year Book.

2.4. Methodology

All of the uncertainty analysis techniques (i.e., ParaSol, SUFI2, and GLUE) used in this study are embedded into a platform—SWAT-CUP [25]—an interface that allows the users to implement the uncertainty analysis for SWAT with multiple-methodological choices. A brief introduction of the three methods is provided in the following sections.

2.4.1. ParaSol

The ParaSol method combines the objective functions (OFs) with a global optimization criterion and implements the simulation and uncertainty analysis using the Shuffle Complex (SCE-UA) algorithm [36]. The SCE-UA is a global search algorithm for the minimization of a specific function [36]. It combines the direct search method of the simplex procedure with the concept of a controlled random search, a systematic evolution of points in the direction of global improvement, competitive evolution, and the concept of complex shuffling [25]. In the operation of SCE-UA, it firstly selects the initial ‘population’ by random sampling to optimize a certain parameter in feasible parameter space. After the optimization, the simulations are divided into behavioral and non-behavioral simulations according to the criterion value. The ParaSol is efficient in seeking the optimal parameters, because the algorithm samples over the entire parameter space with a focus on solutions near the optimum/optima [24]. The method has been widely applied in the uncertainty analysis in the hydrological simulation, especially for the SWAT model.

2.4.2. SUFI2

Based on a Bayesian framework, SUFI2 quantifies the uncertainties through the sequential and fitting processes. In SUFI2, the parameter uncertainty is calculated from all sources such as the indeterminacy of input variables (e.g., rainfall data, temperature and land use), model structure, and measured data (e.g., surface runoff) [12]. The P-factor, the percentage of observed data bracketed by 95% prediction uncertainty (95PPU), is used to quantify the degree of all uncertainties. The 95PPU is calculated at the 2.5% and 97.5% levels of the cumulative distribution of output variables through Latin hypercube sampling method [18]. For streamflow, a value of P-factor > 0.7 or 0.75 has been reported to be adequate, which illustrates most of the observed data within 95PPU band and the model have been well calibrated [18,23,37]. The R-factor is another index to quantify the strength of a calibration and uncertainty analysis and it reflects the average thickness of the 95PPU band divided by the standard deviation of the measured data. Theoretically, a P-factor of 1 and R-factor of 0 indicate that the simulation exactly corresponds to the measured data [18,25]. Further goodness of fit can be quantified by the R^2 and/or Nash-Sutcliffe model efficiency (NSE) between the observations and the best simulation. SUFI2 can currently handle six different objective functions (e.g., two types of root mean square error, Chi square, NSE, R^2 , and bR^2) and the step-by-step operation of SUFI2 can be found in Abbaspour [25].

2.4.3. GLUE

The Generalized Likelihood Uncertainty Estimation (GLUE) method is an uncertainty analysis technique which was introduced by Beven and Binley [26] to allow for the possible non-uniqueness of parameter sets during the estimation in over-parameterized models. The method is used to derive the predictive probability of output variables based on the estimation of the weights or probabilities associated with different parameter sets [26]. In the GLUE operation, it assumes that in the case of the large over-parameterized models, there is no unique set of parameters. In addition, GLUE determines

‘good’ or ‘not good’ simulations by a combination of parameters, and the capability of the GLUE method in uncertainty analysis can also be evaluated by the P-factor and R-factor. GLUE can currently support a likelihood measure expressed as the NSE, and the method has also been increasingly applied in the parameter uncertainty analysis and hydrological simulation.

3. Results

3.1. Global Sensitivity

Based on the previous publications related to hydrological simulation using SWAT [38–40] as well as our own experience [41], we selected six key parameters (see Table 1) to implement sensitivity and uncertainty analysis by using the three methods, and the sensitivity ranks were shown in Figure 2. It is important to point out that we performed 1800 model runs in ParaSol and 2000 model runs in SUFI2 or GLUE. Obviously, the ranks of the six parameters yielded by the three methods showed that CN2 was the most sensitive parameter, followed by SOL_K, and the other four parameters showed relatively less sensitivity for streamflow. To accurately identify the parameter sensitivity towards the streamflow, we also tested the individual effect of the six parameters at three levels—the 25th (1st Quantile), the 50th (medium), and the 75th (3rd Quantile) percentiles of the parameter distributions, and their relationships were shown in Figure 3. For the peak flow, the parameter CN2 showed obviously positive relationship, especially in SUFI2, suggesting that CN2 played a key role in simulating the peak flow in this basin. For the average flow, SOL_K exhibited slightly positive relationship, while others showed no obvious relationships with the average flow. Significantly, the parameter ALPHA_BF negatively correlated with the low flow using the three methods. However, the obvious relationships were not found for other parameters. Additionally, the ranks of the sensitivity and relationships between the streamflow and each parameter yielded by ParaSol, SUFI2, and GLUE demonstrated that all the three methods can be used for parameter sensitivity analysis.

Table 1. Calibrated parameter values for monthly streamflow in the Jingchuan River Basin using Parasol, SUFI2, and GLUE.

| Parameter | Description | Range | Calibrated Value | | |
|------------|---|--------------|------------------|-------|------|
| | | | ParaSol | SUFI2 | GLUE |
| r_CN2 | SCS curve number for soil condition II | −50% to +10% | −46% | −38% | −29% |
| v_ALPHA_BF | Baseflow alpha factor (day) | 0.01–0.1 | 0.04 | 0.05 | 0.04 |
| v_ESCO | Soil evaporation percolation fraction | 0.1–1.0 | 0.93 | 0.5 | 0.16 |
| v_CH_K2 | Effective hydraulic conductivity in main channel alluvium | 8.0–18.0 | 8.0 | 8.4 | 8.06 |
| r_SOL_AWC | Available water capacity of soil layer | −20% to +10% | −17% | 9% | 6% |
| r_SOL_K | Saturated hydraulic conductivity (mm/h) | −10% to +40% | −10% | −4% | −4% |

Note: r means the relative change (%); v means replacing the existing parameter value with the given value.

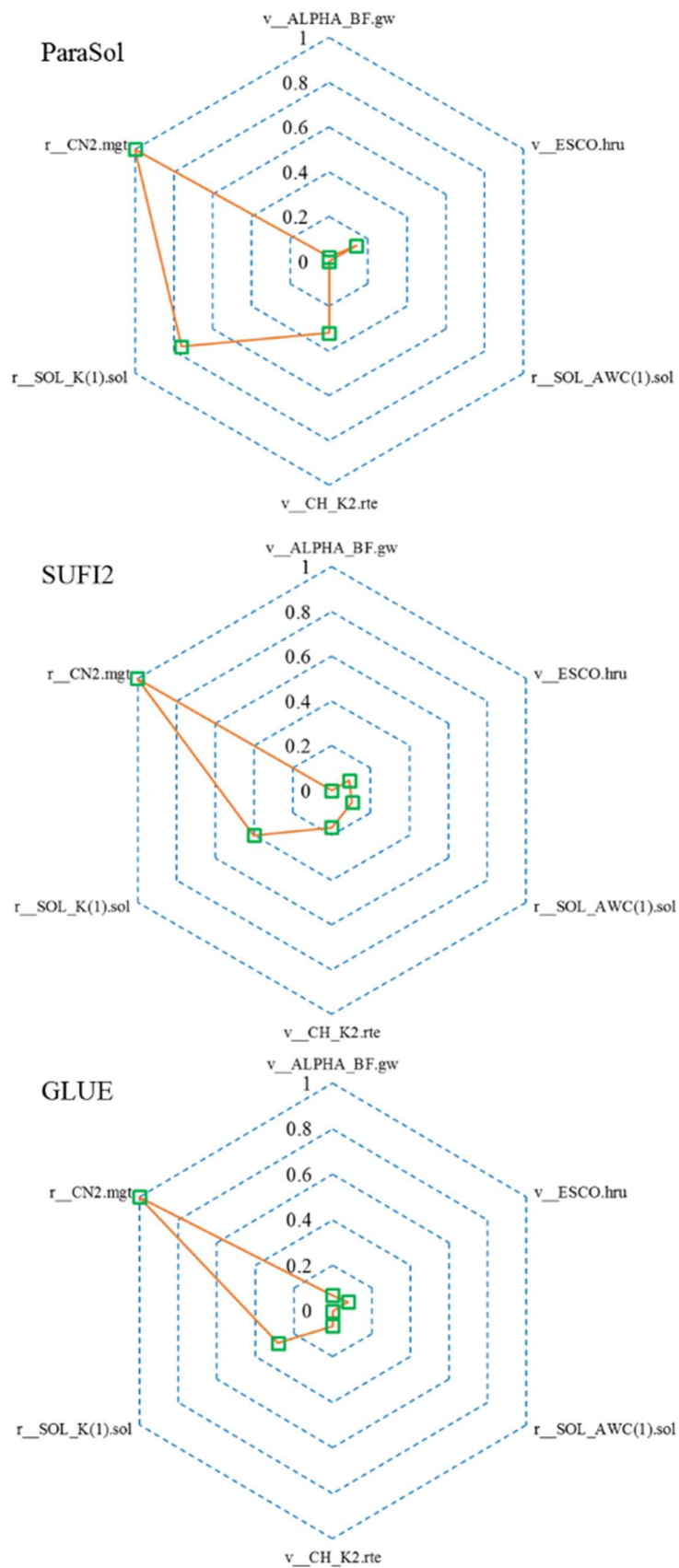


Figure 2. Graphical representation of the parameter sensitivity rank for streamflow yielded by ParaSol, SUFI2, and GLUE. The sensitivity result has been normalized, and a value close to one indicates the parameter is more sensitive to streamflow. The green box means the sensitivity magnitude of a parameter.

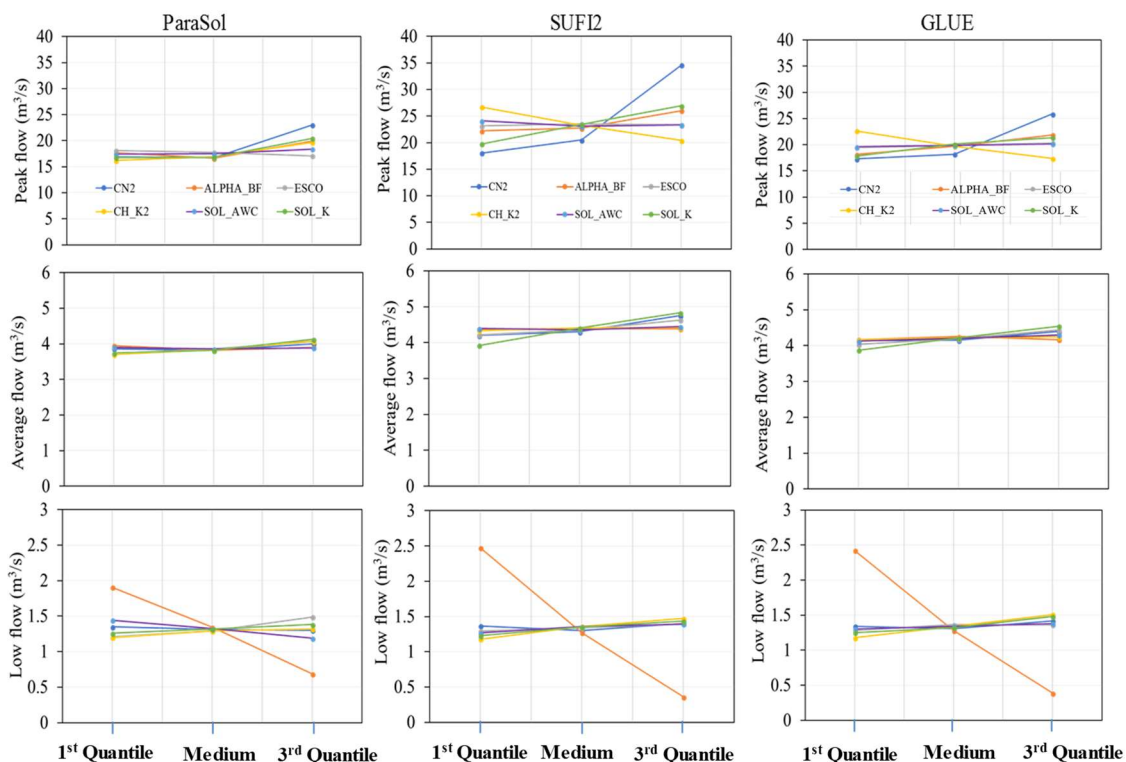


Figure 3. The effect of each parameter generated by the three methods on the peak flow, average flow, and low flow. 1st Quantile, medium, and 3rd Quantile are denoted by 25th, 50th, and 75th percentiles of the parameter distributions, respectively.

3.2. Model Calibration and Validation Results

We compared the capabilities of ParaSol, SUFI2, and GLUE in capturing the optimal parameter sets (in terms of the evaluation criteria) during both the calibration and validation periods in the JCRB. A three-year (2008–2010) record of monthly streamflow at the basin outlet was used for calibration and another two-year (2011–2012) dataset was used for validation. The three sets of the calibrated parameter values derived from the methods were listed in Table 1 and the graphical comparisons (scatterplots) between the observed streamflow and the best simulation were shown in Figure 4. It can be seen from Table 1 and Figure 4 that the calibrated parameter sets of the three methods were not completely in accordance with each other, implying that the three algorithms could recognize the different parameter sets that were able to produce similarly good performance. As can be seen from Table 2, in calibration, the RMSE and RSR yielded by ParaSol (1.24 m³/s and 0.31) were less than those generated by SUFI2 and GLUE (1.3 m³/s and 0.33 for SUFI2 and GLUE, respectively). Also, the NSE and R² in ParaSol (0.90 and 0.91) were higher than those yielded by SUFI2 (0.89 and 0.89) and GLUE (0.89 and 0.89), suggesting that ParaSol had its advantage on accurately seeking the optimized parameter set compared to SUFI2 and GLUE. In addition, based on the evaluation criteria (see Table 2) and according to Moriasi et al. (2007) [42], the overall model performance can be rated as “good” in both the calibration and validation periods.

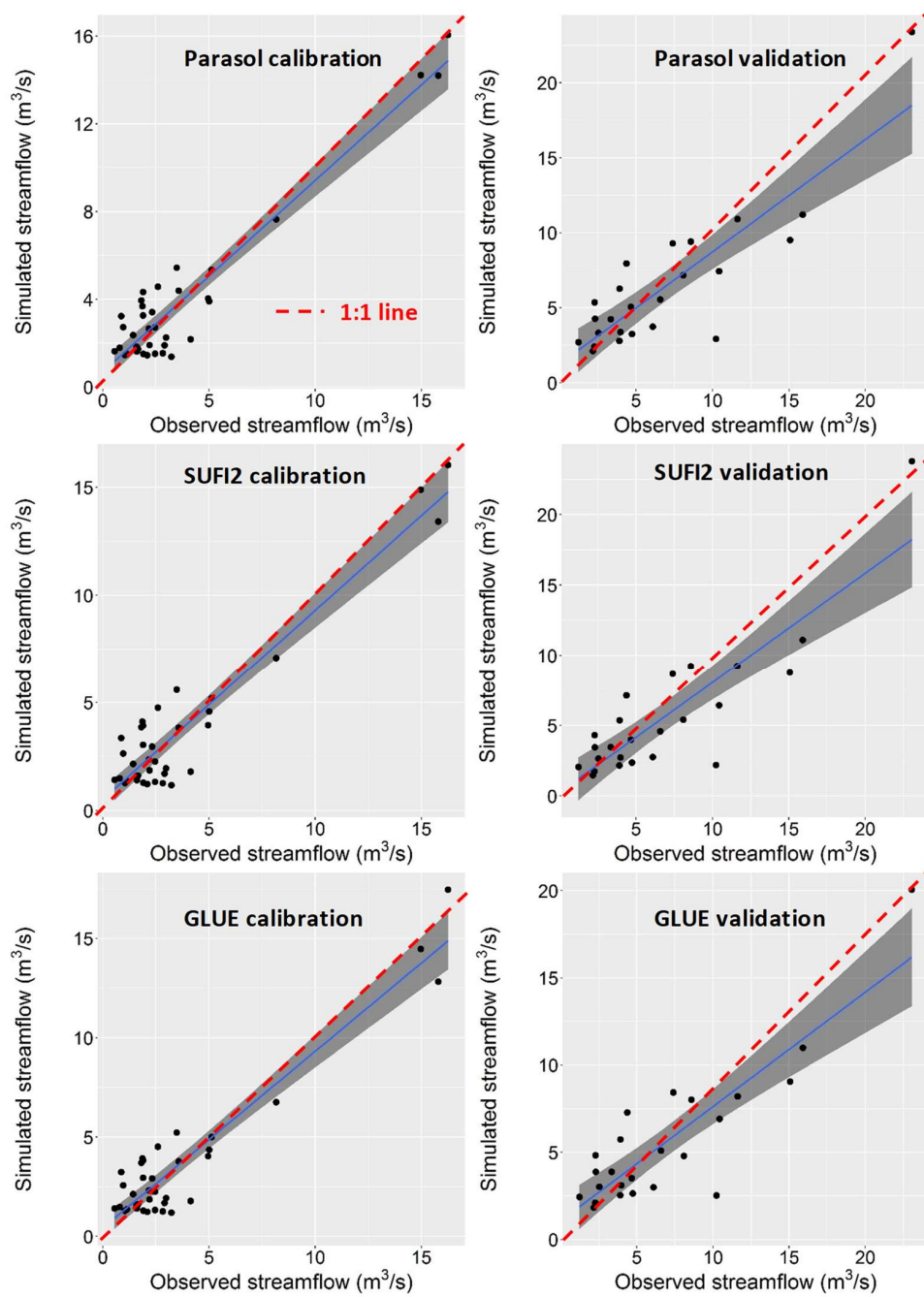


Figure 4. Scatterplots between the best simulation and the observation with the 95% confidence interval (the shaded area).

Table 2. Evaluation of model performance in streamflow simulation during the 3-year (2008–2010) calibration and 2-year (2011–2012) validation periods.

| Method | Period | RMSE (m³/s) | NSE | R ² | RSR | PB (%) |
|---------|-------------|-------------|------|----------------|------|--------|
| ParaSol | Calibration | 1.2 | 0.90 | 0.91 | 0.31 | 6.6 |
| | Validation | 2.6 | 0.74 | 0.75 | 0.50 | −6.8 |
| SUFI2 | Calibration | 1.3 | 0.89 | 0.89 | 0.33 | 2.3 |
| | Validation | 2.9 | 0.69 | 0.75 | 0.54 | −18.2 |
| GLUE | Calibration | 1.3 | 0.89 | 0.89 | 0.33 | 0.9 |
| | Validation | 2.9 | 0.68 | 0.76 | 0.55 | −18.8 |

3.3. Uncertainty Analysis

It is important to point out that the uncertainty analysis was firstly implemented in the calibration period (2008–2010) and then enlarged to validation (2011–2012) due to the short time of the observed data.

3.3.1. Parasol

Implementation of ParaSol is relatively easy and the computation depends only on the convergence of the optimization process. The upper (97.5%) and lower (2.5%) bounds of the posterior parameter values, expressed as the 95% confidence interval (95CI), and the model prediction uncertainty were shown in Table 3 and Figure 5 (top panel), respectively. The 95CI widths for most parameters were narrower than the initial ranges, except for ESCO and SOL_AWC. Since the optimal values of the latter parameters remained either at the lower or at the upper bounds (see Table 3), indicating that ESCO and SOL_AWC were more uncertain. In general, a higher P-factor means more observations fall inside 95PPU. As can be seen from Figure 5, the uncertainty band was very narrow and the P-factor was only 0.39 and 0.46 in the calibration and validation periods, respectively. This demonstrated that ParaSol had the limited ability for conducting uncertainty analysis though the best simulation matched the observation very well with good NSE and R^2 . Figure 6a, b showed the distribution of the model response as a function of the parameter values and the change of standard residuals following the simulated streamflow. It was significant that there existed an overestimation of prediction uncertainty in the wet month (high streamflow), suggesting that more attention should be paid to the wet season in the hydrological simulation. This phenomenon can also be seen from Figure 5 (top panel), where the width of 95PPU band was relatively larger in the high-rainfall seasons. Also, the variance of the residuals was not constant and changed with the streamflow, and this may illustrate that there existed heteroscedasticity in ParaSol. In addition, the correlation matrix showed relatively strong correlations (r ranging from -0.40 to 0.57) among the model parameters, especially the $r_{\text{SOL_K}}$ and $v_{\text{CH_K2}}$ ($r = 0.57$), the $v_{\text{CH_K2}}$ and r_{CN2} ($r = 0.48$).

3.3.2. SUFI2

The SUFI2 method is also convenient to use, though it is semi-distributed and needed for some knowledge of parameters' effects on model output. For the SUFI2 approach, we did one iteration with 2000 model runs using the same parameter ranges for the sake of comparison of the three methods. The 95CI of most parameters yielded by SUFI2 showed a narrower range, though the parameter ALPHA_BF was the same as the initial setting (Table 3), suggesting ALPHA_BF was more uncertain in SUFI2. For the model prediction, it can be seen from Figure 5 (medium panel) that the 95PPU bracketed 83% and 71% of the observations in the calibration and validation periods, respectively, illustrating that SUFI2 was more capable of capturing the observations in spite of a large R-factor. Further, the 95PPU was more suitable to bracket the observations of year 2010, while it slightly overestimated the runoff in winter seasons of year 2008 and 2009. For validation, it underestimated the streamflow from the autumn in 2011 to the summer in 2012, resulting in a relatively poor performance. Similarly, the sensitivity range (Figure 6c) also indicated that the effect of parameter on model outcome was relatively higher in wet seasons (i.e., months with high precipitation). This may be attributed to the uncertainty involved in computing baseflow recession in SWAT and the coarse observations [27]. The residuals were also not normally distributed with constant variance (Figure 6d), which may lead to biased parameter estimation due to the systematic error [43,44]. In addition, the correlation matrix (Table 4) showed very weak correlations among the parameters, and thus, the parameter correlations can be neglected in SUFI2.

Table 3. Uncertainty ranges of aggregate parameters from the three methods.

| Parameter | Initial Range | 95CI (Confidence Interval) | | |
|------------|---------------|----------------------------|--------------|--------------|
| | | ParaSol | SUF12 | GLUE |
| r_CN2 | −50% to +10% | (−48.0, 0.2) | (−48.5, 8.5) | (−48.5, 8.5) |
| v_ALPHA_BF | 0.01–0.1 | (0.01, 0.09) | (0.01, 0.1) | (0.01, 0.1) |
| v_ESCO | 0.1–1.0 | (0.14, 0.98) | (0.13, 0.98) | (0.12, 0.98) |
| v_CH_K2 | 8.0–18.0 | (8.5, 16.7) | (8.3, 17.7) | (8.3, 17.7) |
| r_SOL_AWC | −20% to +10% | (−18.2, 8.5) | (−19.2, 9.2) | (−19.2, 9.2) |
| r_SOL_K | −10% to +40% | (−8.9, 29.5) | (−8.7, 38.7) | (−8.7, 38.7) |

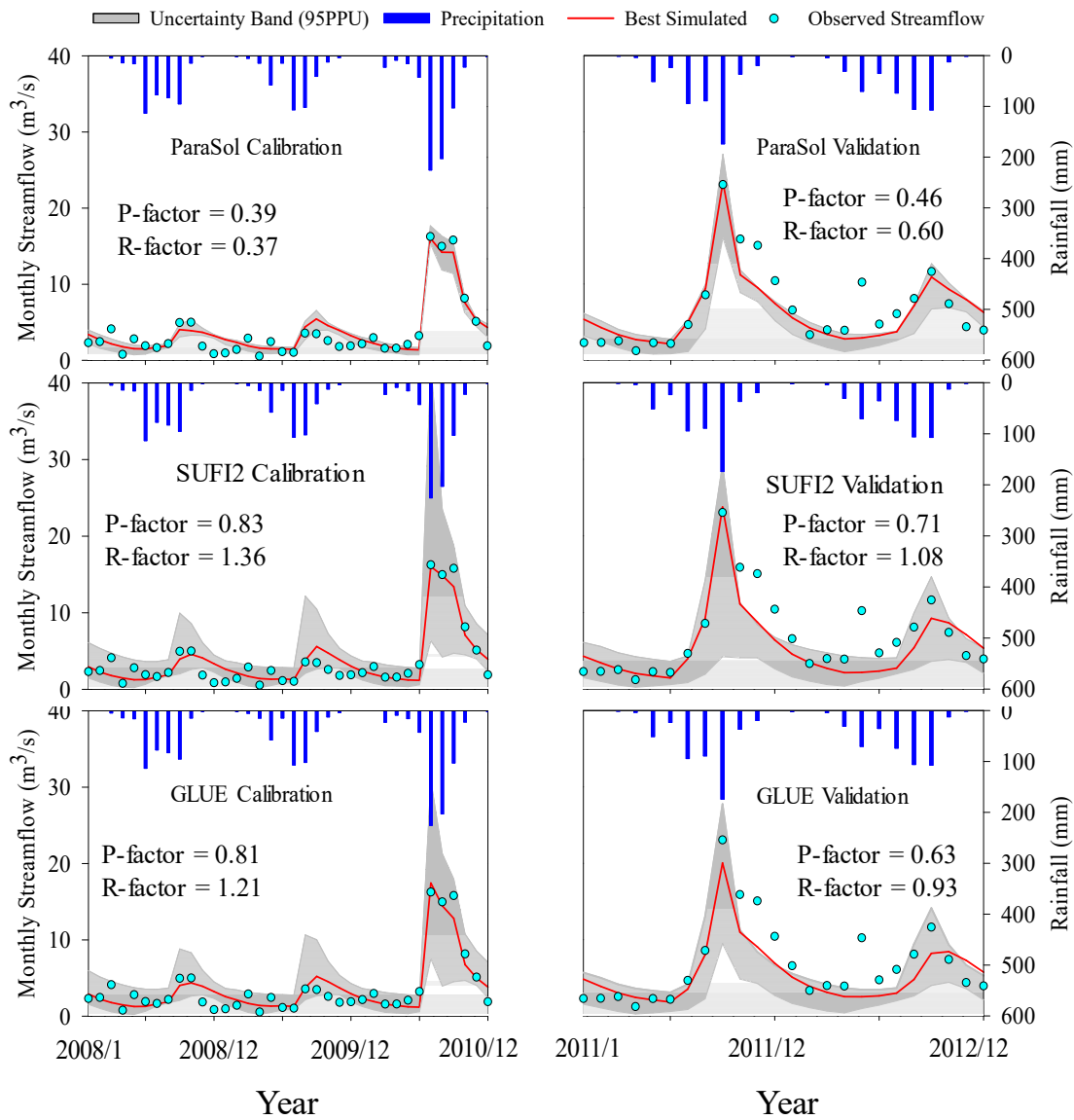


Figure 5. Comparison of best-simulated monthly streamflow with 95PPU against observed streamflow by ParaSol (top), SUF12 (medium), and GLUE (bottom). P-factor indicates the percentage of observed data bracketed by 95% prediction uncertainty; R-factor reflects the average thickness of 95PPU band divided by the standard deviation of the measured data.

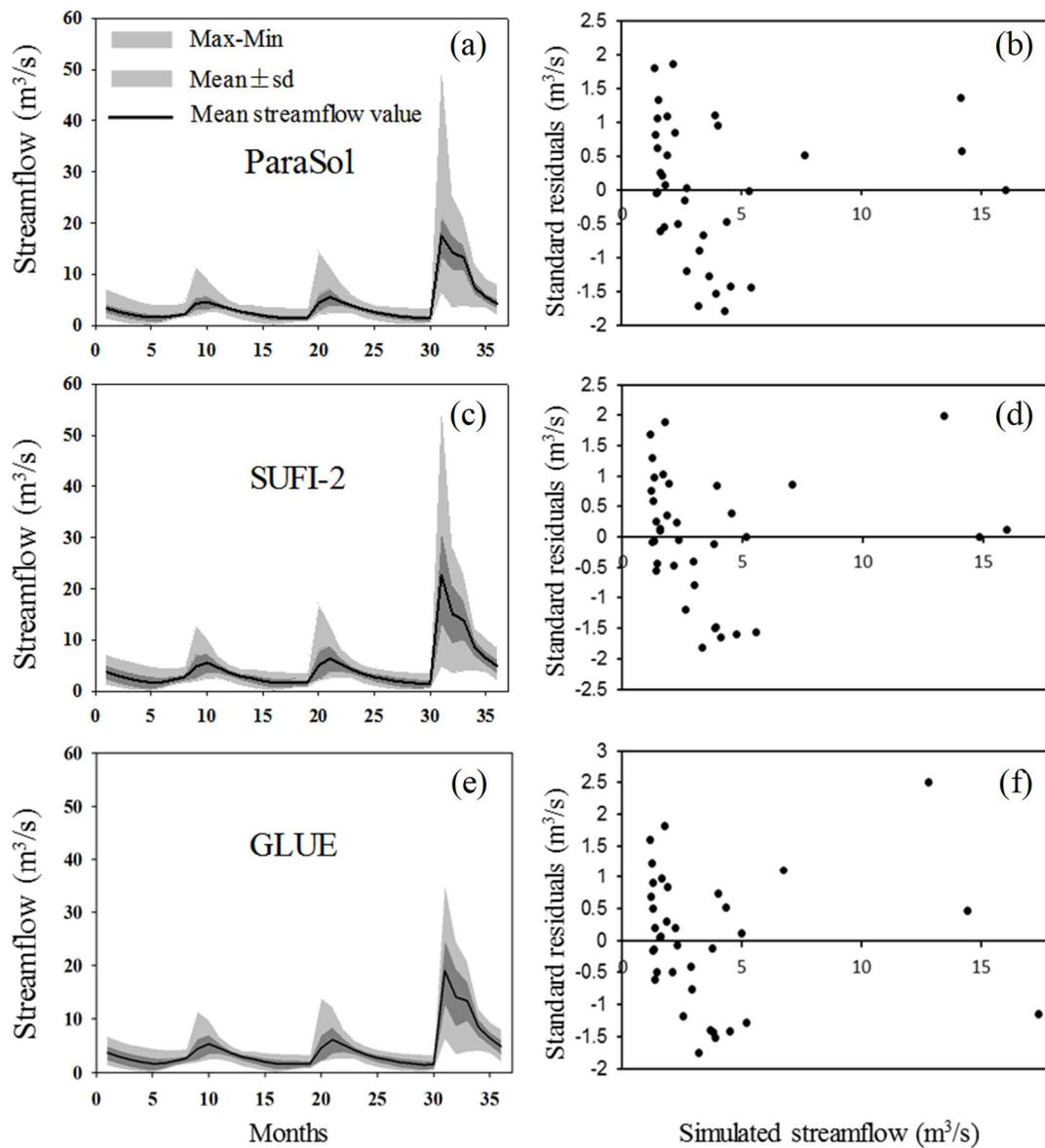


Figure 6. Sensitivity range of monthly streamflow (left column) based on the parameter distribution as generated by ParaSol (a), SUFI2 (c) and GLUE (e) during the 3-year calibration (2008–2010), sd refers to the standard deviation of the model response. The light grey shade by Mine-Max represents the minimum and maximum model response at each time step, whereas the dark grey shade by Mean ± sd refers to the mean model response plus/minus one standard deviation. The right column indicates the standard residuals versus simulated streamflow obtained from ParaSol (b), SUFI2 (d) and GLUE (f) during the calibration period.

3.3.3. GLUE

GLUE is convenient and easy to use and has been widely applied in hydrological field. We also did 2000 runs in GLUE implementation within the same parameter ranges to compare the capabilities of the three methods in parameter uncertainty analysis. The 95CI showed that the parameter uncertainty ranges generated by GLUE were similar with those yielded by SUFI2 but obviously larger than ParaSol, especially for CN2 and SOL_K (Table 3). It can be seen from Figure 5 (bottom panel) that 81% of the observations were bracketed by the 95PPU and the R-factor equaled 1.21 in calibration, which was similar to SUFI2, suggesting that GLUE was also able to capture the observations in calibration. In validation, 63% of the observations were bracketed by the 95PPU, which was slightly less than

SUFI2. Also, GLUE overestimated the streamflow in the winter seasons of year 2008 and 2009, while it somewhat underestimated the streamflow of year 2012. The parameter uncertainty was also found to be higher in the wet seasons during the calibration period (see Figure 6e). The change of residuals demonstrated that the parameter uncertainty estimation may be somewhat biased (Figure 6f). Similar to SUFI2, there was almost no correlations among the parameters yielded by GLUE, and thus the parameter correlations could also be neglected in GLUE.

Table 4. Correlation matrix of the streamflow parameters yielded by ParaSol, SUFI2, and GLUE.

| Method | Parameter | r_CN2 | v_ALPHA_BF | v_ESCO | v_CH_K2 | r_SOL_AWC | r_SOL_K |
|---------|------------|-------|------------|--------|---------|-----------|---------|
| ParaSol | r_CN2 | 1 | 0.11 | −0.24 | 0.48 | 0.11 | 0.37 |
| | v_ALPHA_BF | | 1 | −0.27 | 0.27 | 0.25 | 0.21 |
| | v_ESCO | | | 1 | −0.24 | −0.40 | −0.25 |
| | v_CH_K2 | | | | 1 | 0.20 | 0.57 |
| | r_SOL_AWC | | | | | 1 | 0.15 |
| | r_SOL_K | | | | | | 1 |
| SUFI2 | r_CN2 | 1 | −0.01 | 0.02 | −0.02 | −0.02 | −0.02 |
| | v_ALPHA_BF | | 1 | 0.01 | 0.02 | −0.03 | −0.02 |
| | v_ESCO | | | 1 | 0.03 | −0.00 | −0.00 |
| | v_CH_K2 | | | | 1 | −0.02 | −0.02 |
| | r_SOL_AWC | | | | | 1 | 0.03 |
| | r_SOL_K | | | | | | 1 |
| GLUE | r_CN2 | 1 | −0.02 | −0.03 | −0.02 | 0.01 | −0.02 |
| | v_ALPHA_BF | | 1 | 0.01 | 0.02 | −0.02 | −0.01 |
| | v_ESCO | | | 1 | 0.01 | −0.01 | −0.00 |
| | v_CH_K2 | | | | 1 | 0.03 | 0.01 |
| | r_SOL_AWC | | | | | 1 | −0.00 |
| | r_SOL_K | | | | | | 1 |

4. Discussion

4.1. Model Parameterization and Performance

For a better streamflow simulation, the accurate identification of key parameters is important. In this study, we identified six key parameters related to streamflow simulation by using the three popular methods in the JCRB. As can be seen from Table 1, ParaSol provided the least CN2, SOL_AWC, and SOL_K values compared to those yielded by SUFI2 and GLUE. Most of the parameter values generated by SUFI2 were similar with those yielded by GLUE. The phenomenon may be attributed to the objective functions of the methods and the initial parameters' ranges. In our study, the objective function in ParaSol was limited to the sum of the squares of the residuals [25], indicating that ParaSol aimed to find the least bias when seeking the best parameter set. However, the NSE was the objective function in both SUFI2 and GLUE, which may handle a different pathway in finding the best fitting parameter set. In addition, the initial parameter ranges may also play an important role in seeking appropriate parameter sets because the initial ranges can decide both the parameters' combination and applicability. Therefore, the above conditions may result in different calibrated parameter values using the three methods.

The comparisons of the SWAT model performance generated by the three methods were listed in Table 2. In terms of the evaluation criteria, ParaSol provided slightly higher NSE and R^2 and achieved less predicting errors (see Table 2) in both the calibration and validation periods, showing its advantage in accurately capturing the optimal parameter set, which was also confirmed by others [1,14,27]. This is because ParaSol is based on the global optimization algorithms and thus samples over the entire parameter space with a focus on solutions near the optimum [45]. This algorithm is much more efficient in finding the maximum or minimum of the objective function than random or Latin hypercube sampling [27,46]. Therefore, ParaSol can be a reasonable choice in seeking the best parameter set in hydrological modeling.

4.2. Parameter Sensitivity and Uncertainty

For parameter sensitivity, the results showed that the parameter CN2 was the most sensitive (Figure 2) using any of the three methods and CN2 played a key role in peak flow simulation (Figure 3). CN2 is a function of soil's permeability, land use, and initial soil water condition, which suggests the potential of surface runoff from rainfall in a watershed [47]. CN2 had positive effects on the peak flow (Figure 3), and this may be because of concentrated distribution of rainfall in the wet season, causing infiltration exceeded surface flow and a significant increase in peak flow. The parameter SOL_K, which represents soil hydraulic conductivity and closely relates to the movement of water in soil profiles, had a positive effect on average streamflow. In the study area, Cambisols is widely distributed (see Figure 1) and is mainly made up of sandy loam that is characterized with medium percolation capacity. Water in this soil can be easier to percolate to the shallow aquifer and further contributed to the baseflow and then the streamflow. ALPHA_BF is the baseflow recession factor, a high value of ALPHA_BF means quick recession of baseflow (i.e., the less water retention in the aquifer), and this was why this parameter played a key role in the relationship between the low flow and ALPHA_BF.

For parameter uncertainty, our study showed that GLUE and SUFI2 provided the wider 95CIs than ParaSol (see Table 3). Most of the uncertainty intervals derived by GLUE and SUFI2 contained the corresponding intervals from ParaSol. Based on SCE-UA, ParaSol was very efficient in seeking the most suitable parameter set near the maximum or minimum objective function value [27], which suggested that the parameter can be narrowed to a relatively small extent. The wider parameter ranges in SUFI2 and GLUE may be because they considered all sources of uncertainty and thus may lead to relatively larger ranges of parameter uncertainty [46]. As we know, the GLUE method considers the parameter correlation in uncertainty analysis, but Table 4 showed that there were almost no correlations among the parameters, which was the same as SUFI2. Therefore, through the comparisons of the parameter uncertainty ranges as well as the parameter correlations, both SUFI2 and GLUE showed advantages in providing similarly good parameter uncertainty ranges [1,12,14,27].

4.3. Model Prediction Uncertainty

For model prediction uncertainty analysis, we found that SUFI2 was a superior tool because of its relatively larger P-factor and reasonable R-factor. As seen from Figure 5, ParaSol did not derive reasonable prediction uncertainty and only 39% and 46% measurements were bracketed by the 95PPU in calibration and validation, respectively, in spite of the good R^2 and NSE. This was because ParaSol does not consider the error in the measured data, model structure, and measured response, leading to an underestimation of the prediction uncertainty [17,27]. As stated previously, the parameter uncertainty yielded by Parasol only accounted for a small part of the whole uncertainty; whereas, SUFI2 and GLUE took into account all sources of uncertainties, and the corresponding parameter ranges (95CI) were also larger than ParaSol, leading to the wider 95PPU bands. In addition, according to Abbaspour et al. [18], the 95PPU should bracket at least 80% of the observed data if the measurements are of high quality. In terms of our results, SUFI2 and GLUE bracketed above 80% of the observed streamflow in the calibration period, although we recognized that there still existed a certain uncertainty in SWAT (1.36 and 1.21 of R-factor in SUFI2 and GLUE, respectively), which may be because of the overestimation of the errors in the input, output, and model structure. It was also worth noting that the coverage (P-factor) of GLUE can be increased at the expense of increasing R-factor, and in SUFI2 this can be done by performing one more iteration. Compared to GLUE, the 95PPU in SUFI2 bracketed 83% and 71% measurements in calibration and validation, respectively, suggesting that SUFI2 was more capable of capturing the observations. The main reason could be all these sampled parameter sets were taken as behavioral samples and contributed to the 95PPU [12]. Additionally, based on the previous studies and our own experience [1,14,16,27], the SUFI2 method has a high efficiency in computation because of the advantages in taking into account the discrete parameter space of the Latin hypercube sampling [27]. In contrast, GLUE makes use of the Monte Carlo simulation for random sampling and needs a certain number of sampling runs to derive the most

reasonable outputs, especially for the complex models [6,12,14]. Therefore, SUFI2 is more efficient for uncertainty analysis in the hydrological simulation when handling some high dimensional and complex hydrological models.

5. Conclusions

This study examined the capabilities of three uncertainty analysis methods through a distributed hydrological model—SWAT with a case study in the JCRB on the Chinese Loess Plateau. The modeling results showed that the SWAT model was acceptable in the streamflow simulation in the JCRB with NSE and R^2 being 0.90 and 0.91 for calibration, and 0.74 and 0.75 for validation, respectively. The sensitivity analysis of the selected six key parameters indicated that ParaSol, SUFI2, and GLUE could be used for parameter sensitivity analysis in the study area. The sensitivity results showed that CN2, SOL_K, and ALPHA_BF were more sensitive to the simulation of peak flow, average flow, and low flow, respectively, compared to others (e.g., ESCO, CH_K2, and SOL_AWC) in this area. Although ParaSol was more efficient in capturing the optimal parameter set, it did not derive the suitable parameter and prediction uncertainty ranges due to its relatively narrower 95CI and poor P-factor and R-factor. Compared to ParaSol, SUFI2 and GLUE were proven to be more capable in predicting the parameter uncertainty, and SUFI2 was superior to GLUE in terms of the P-factor and R-factor. In summary, through the comparisons of the evaluation criteria for uncertainty analysis (e.g., P-factor, R-factor, NSE, and R^2) and the computational efficiencies, the SUFI2 method performed better than the other two methods for the parameter uncertainty analysis of the SWAT model in the JCRB. The study provides an insight into the identifiability of more reliable methods for uncertainty analysis, especially in the hydrological modeling community.

Finally, although this study was informative by implementing the three popular parameter uncertainty analysis methods, the generality of such findings is to be evaluated with more applications in other areas. Moreover, in addition to the parameters' uncertainty, the uncertainty in model structure and input data should be examined for the complete and deep understanding of the modeling behavior.

Author Contributions: F.Z. and Y.W. designed and performed the study, interpreted the results, and wrote the paper. L.Q., Y.S., L.S., Q.L., J.N. and G.W. contributed to data collection, results presentation, and draft revision.

Funding: This study was funded by the National Thousand Youth Talent Program of China, the Hundred Youth Talent Program of Shaanxi Province, the Young Talent Support Plan of Xi'an Jiaotong University, National Natural Science Foundation of China (31741020), National Key Research and Development Project (2016YFA0601501), and Natural Science Foundation of Guangdong Province (2016A050503035).

Conflicts of Interest: The authors declare no conflict of interest.

References

1. Uniyal, B.; Jha, M.K.; Verma, A.K. Parameter identification and uncertainty analysis for simulating streamflow in a river basin of eastern India. *Hydrol. Process.* **2015**, *29*, 3744–3766. [[CrossRef](#)]
2. Gyamfi, C.; Ndambuki, J.; Salim, R. Hydrological responses to land use/cover changes in the Olifants Basin, South Africa. *Water* **2016**, *8*, 588. [[CrossRef](#)]
3. Viviroli, D.; Zappa, M.; Gurtz, J.; Weingartner, R. An introduction to the hydrological modelling system prevah and its pre- and post-processing-tools. *Environ. Model. Softw.* **2009**, *24*, 1209–1222. [[CrossRef](#)]
4. Wu, K.; Xu, Y.J. Evaluation of the applicability of the SWAT model for coastal watersheds in southeastern Louisiana. *J. Am. Water Resour. Assoc.* **2006**, *42*, 1247–1260. [[CrossRef](#)]
5. Zhu, X.; Zhang, C.; Qi, W.; Cai, W.; Zhao, X.; Wang, X. Multiple climate change scenarios and runoff response in Biliu River. *Water* **2018**, *10*, 126. [[CrossRef](#)]
6. Beven, K.; Freer, J. Equifinality, data assimilation, and uncertainty estimation in mechanistic modelling of complex environmental systems using the glue methodology. *J. Hydrol.* **2001**, *249*, 11–29. [[CrossRef](#)]
7. Zheng, Y.; Han, F. Markov Chain Monte Carlo (MCMC) uncertainty analysis for watershed water quality modeling and management. *Stoch. Environ. Res. Risk Assess.* **2015**, *30*, 293–308. [[CrossRef](#)]

8. Li, Z.; Xu, Z.; Shao, Q.; Yang, J. Parameter estimation and uncertainty analysis of SWAT model in upper reaches of the Heihe River Basin. *Hydrol. Process.* **2009**, *23*, 2744–2753. [[CrossRef](#)]
9. Song, X.; Zhang, J.; Zhan, C.; Xuan, Y.; Ye, M.; Xu, C. Global sensitivity analysis in hydrological modeling: Review of concepts, methods, theoretical framework, and applications. *J. Hydrol.* **2015**, *523*, 739–757. [[CrossRef](#)]
10. Li, Z.; Shao, Q.; Xu, Z.; Cai, X. Analysis of parameter uncertainty in semi-distributed hydrological models using bootstrap method: A case study of SWAT model applied to Yingluoxia watershed in Northwest China. *J. Hydrol.* **2010**, *385*, 76–83. [[CrossRef](#)]
11. Yen, H.; Wang, X.; Fontane, D.G.; Harmel, R.D.; Arabi, M. A framework for propagation of uncertainty contributed by parameterization, input data, model structure, and calibration/validation data in watershed modeling. *Environ. Model. Softw.* **2014**, *54*, 211–221. [[CrossRef](#)]
12. Xue, C.; Chen, B.; Asce, M.; Wu, H. Parameter uncertainty analysis of surface flow and sediment yield in the Huolin Basin, China. *J. Hydrol. Eng.* **2014**, *19*, 1224–1236. [[CrossRef](#)]
13. Refsgaard, J.C.; van der Sluijs, J.P.; Brown, J.; van der Keur, P. A framework for dealing with uncertainty due to model structure error. *Adv. Water Res.* **2006**, *29*, 1586–1597. [[CrossRef](#)]
14. Wu, H.; Chen, B. Evaluating uncertainty estimates in distributed hydrological modeling for the Wenjing River watershed in China by GLUE, SUFI-2, and ParaSol methods. *Ecol. Eng.* **2015**, *76*, 110–121. [[CrossRef](#)]
15. Nandakumar, N.; Mein, R.G. Uncertainty in rainfall-runoff model simulations and the implications for predicting the hydrologic effects of land-use change. *J. Hydrol.* **1997**, *193*, 211–232. [[CrossRef](#)]
16. Zhou, J.; Liu, Y.; Guo, H.; He, D. Combining the SWAT model with sequential uncertainty fitting algorithm for streamflow prediction and uncertainty analysis for the lake Dianchi Basin, China. *Hydrol. Process.* **2014**, *28*, 521–533. [[CrossRef](#)]
17. Zhang, J.; Li, Q.; Guo, B.; Gong, H. The comparative study of multi-site uncertainty evaluation method based on SWAT model. *Hydrol. Process.* **2015**, *29*, 2994–3009. [[CrossRef](#)]
18. Abbaspour, K.C.; Yang, J.; Maximov, I.; Siber, R.; Bogner, K.; Mieleitner, J.; Zobrist, J.; Srinivasan, R. Modelling hydrology and water quality in the pre-alpine/alpine Thur watershed using SWAT. *J. Hydrol.* **2007**, *333*, 413–430. [[CrossRef](#)]
19. Vilaysane, B.; Takara, K.; Luo, P.; Akkharath, I.; Duan, W. Hydrological stream flow modelling for calibration and uncertainty analysis using SWAT model in the Xedone River Basin, Lao PDR. *Procedia Environ. Sci.* **2015**, *28*, 380–390. [[CrossRef](#)]
20. Zhang, X.; Srinivasan, R.; Bosch, D. Calibration and uncertainty analysis of the swat model using Genetic Algorithms and Bayesian Model Averaging. *J. Hydrol.* **2009**, *374*, 307–317. [[CrossRef](#)]
21. Wu, Y.; Liu, S. Automating calibration, sensitivity and uncertainty analysis of complex models using the R package Flexible Modeling Environment (FME): SWAT as an example. *Environ. Model. Softw.* **2012**, *31*, 99–109. [[CrossRef](#)]
22. Wu, Y.; Liu, S.; Yan, W. A universal model-R coupler to facilitate the use of r functions for model calibration and analysis. *Environ. Model. Softw.* **2014**, *62*, 65–69. [[CrossRef](#)]
23. Abbaspour, K.C.; Rouholahnejad, E.; Vaghef, S.; Srinivasan, R.; Yang, H.; Kløve, B. A continental-scale hydrology and water quality model for Europe: Calibration and uncertainty of a high-resolution large-scale SWAT model. *J. Hydrol.* **2015**, *524*, 733–752. [[CrossRef](#)]
24. van Griensven, A.; Meixner, T. Methods to quantify and identify the sources of uncertainty for river basin water quality models. *Water Sci. Technol.* **2006**, *53*, 51–59. [[CrossRef](#)] [[PubMed](#)]
25. Abbaspour, K.C. *SWAT Calibration and Uncertainty Programs: A User Manual*; Swiss Federal Institute of Aquatic Science and Technology (Eawag): Dübendorf, Switzerland, 2011.
26. Beven, K.; Binley, A. The future of distributed models-model calibration and uncertainty prediction. *Hydrol. Process.* **1992**, *6*, 279–298. [[CrossRef](#)]
27. Yang, J.; Reichert, P.; Abbaspour, K.C.; Xia, J.; Yang, H. Comparing uncertainty analysis techniques for a SWAT application to the Chaohe Basin in China. *J. Hydrol.* **2008**, *358*, 1–23. [[CrossRef](#)]
28. Khalid, K.; Ali, M.F.; Rahman, N.F.A.; Mispan, M.R.; Haron, S.H.; Othman, Z.; Bachok, M.F. Sensitivity analysis in watershed model using SUFI-2 algorithm. *Procedia Eng.* **2016**, *162*, 441–447. [[CrossRef](#)]
29. Kouchi, D.H.; Esmaili, K.; Faridhosseini, A.; Sanaeinejad, S.H.; Khalili, D.; Abbaspour, K.C. Sensitivity of calibrated parameters and water resource estimates on different objective functions and optimization algorithms. *Water* **2017**, *9*, 384. [[CrossRef](#)]

30. Arnold, J.G.; Srinivasn, R.; Muttiah, R.S.; Willians, J.R. Large area hydrologic modeling and assessment—Part I: Model development. *J. Am. Water Resour. Assoc.* **1998**, *34*, 73–89. [[CrossRef](#)]
31. Zhang, L.; Podlasly, C.; Feger, K.-H.; Wang, Y.; Schwärzel, K. Different land management measures and climate change impacts on the runoff—A simple empirical method derived in a mesoscale catchment on the loess plateau. *J. Arid Environ.* **2015**, *120*, 42–50. [[CrossRef](#)]
32. Neitsch, S.L.; Arnold, J.G.; Kiniry, J.R.; Williams, J.R. *Soil and Water Assessment Tool Theoretical Documentation Version 2009*; Texas Water Resources Institute: Ollege Station, TX, USA, 2011.
33. Panagopoulos, Y.; Gassman, P.W.; Arritt, R.W.; Herzmann, D.E.; Campbell, T.D.; Valcu, A.; Jha, M.K.; Kling, C.L.; Srinivasan, R.; White, M.; et al. Impacts of climate change on hydrology, water quality and crop productivity in the Ohio-Tennessee River Basin. *Int. J. Agric. Biol. Eng.* **2015**, *8*, 36–53.
34. Arnold, J.G.; Muttiah, R.S.; Srinivasan, R.; Allen, P.M. Regional estimation of base flow and groundwater recharge in the upper Mississippi River Basin. *J. Hydrol.* **2000**, *227*, 21–40. [[CrossRef](#)]
35. Meng, X.; Wang, H. Significance of the china meteorological assimilation driving datasets for the SWAT model (CMADS) of East Asia. *Water* **2017**, *9*, 765. [[CrossRef](#)]
36. Duan, Q.; Sorooshian, S.; Gupta, V. Effective and efficient global optimization for conceptual rainfall-runoff models. *Water Resour. Manag.* **1992**, *28*, 1015–1031. [[CrossRef](#)]
37. Ashraf Vaghefi, S.; Abbaspour, K.; Faramarzi, M.; Srinivasan, R.; Arnold, J. Modeling crop water productivity using a coupled SWAT–MODSIM model. *Water* **2017**, *9*, 157. [[CrossRef](#)]
38. Li, Z.; Liu, W.-Z.; Zhang, X.-C.; Zheng, F.-L. Impacts of land use change and climate variability on hydrology in an agricultural catchment on the Loess Plateau of China. *J. Hydrol.* **2009**, *377*, 35–42. [[CrossRef](#)]
39. Wang, H.; Sun, F.; Xia, J.; Liu, W. Impact of lucc on streamflow based on the SWAT model over the Wei River Basin on the Loess Plateau in China. *Hydrol. Earth Syst. Sci.* **2017**, *21*, 1929–1945. [[CrossRef](#)]
40. Zuo, D.; Xu, Z.; Peng, D.; Song, J.; Cheng, L.; Wei, S.; Abbaspour, K.C.; Yang, H. Simulating spatiotemporal variability of blue and green water resources availability with uncertainty analysis. *Hydrol. Process.* **2015**, *29*, 1942–1955. [[CrossRef](#)]
41. Zhao, F.; Wu, Y.; Qiu, L.; Bellie, S.; Zhang, F.; Sun, Y.; Sun, L.; Li, Q.; Alexey, V. Spatiotemporal features of the hydro-biogeochemical cycles in a typical loess gully watershed. *Ecol. Indic.* **2018**, *91*, 542–554. [[CrossRef](#)]
42. Moriasi, D.N.; Arnold, J.G.; Van Liew, M.W.; Bingner, R.L.; Harmel, R.D.; Veith, T.L. Model evaluation guidelines for systematic quantification of accuracy in watershed simulations. *Trans. ASABE* **2007**, *50*, 885–900. [[CrossRef](#)]
43. Datta, A.R.; Bolisetti, T. Second-order autoregressive model-based likelihood function for calibration and uncertainty analysis of SWAT model. *J. Hydrol. Eng.* **2015**, *20*, 04014045. [[CrossRef](#)]
44. Neupane, R.P.; Kumar, S. Estimating the effects of potential climate and land use changes on hydrologic processes of a large agriculture dominated watershed. *J. Hydrol.* **2015**, *529*, 418–429. [[CrossRef](#)]
45. Van Griensven, A.; Meixner, T.; Grunwald, S.; Bishop, T.; Di luzio, M.; Srinivasan, R. A global sensitivity analysis tool for the paramters of multi-variable catchment models. *J. Hydrol.* **2006**, *324*, 10–23. [[CrossRef](#)]
46. Abbaspour, K.; Vaghefi, S.; Srinivasan, R. A guideline for successful calibration and uncertainty analysis for soil and water assessment: A review of papers from the 2016 International SWAT Conference. *Water* **2017**, *10*, 6. [[CrossRef](#)]
47. Liu, Y.R.; Li, Y.P.; Huang, G.H.; Zhang, J.L.; Fan, Y.R. A bayesian-based multilevel factorial analysis method for analyzing parameter uncertainty of hydrological model. *J. Hydrol.* **2017**, *553*, 750–762. [[CrossRef](#)]

